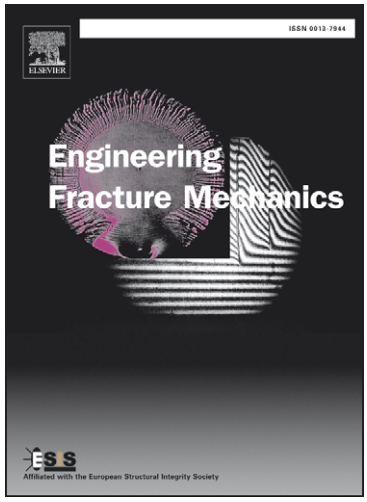

Technical note

The Theory of Critical Distances as an alternative experimental strategy for the determination of K_{Ic} and ΔK_{th}

Luca Susmel, David Taylor

PII: S0013-7944(10)00202-X
DOI: 10.1016/j.engfracmech.2010.04.016
Reference: EFM 3263

To appear in: *Engineering Fracture Mechanics*

Received Date: 27 February 2009
Revised Date: 11 April 2010
Accepted Date: 19 April 2010

Please cite this article as: Susmel, L., Taylor, D., The Theory of Critical Distances as an alternative experimental strategy for the determination of K_{Ic} and ΔK_{th}, *Engineering Fracture Mechanics* (2010), doi: 10.1016/j.engfracmech.2010.04.016

The Theory of Critical Distances as an alternative experimental strategy for the determination of K_{Ic} and ΔK_{th}

- Technical note -

Luca Susmel[1] *and David Taylor*[2]
[1]Department of Engineering, University of Ferrara, Via Saragat 1 – 44100 Ferrara, Italy
[2]Department of Mechanical Engineering, Trinity College, Dublin 2, Ireland

ABSTRACT

The present technical note is concerned with the use of the Theory of Critical Distances, applied in the form of the Point Method, to estimate the range of the threshold value of the stress intensity factor, ΔK_{th}, as well as the plane strain fracture toughness, K_{Ic}, of conventional engineering materials. In more detail, it is shown that ΔK_{th} can efficiently be evaluated by measuring two fatigue limits: the fatigue limit plain (unnotched) specimens and a second fatigue limit generated by testing samples containing a stress concentration feature such as a notch. The K_{Ic}, on the other hand, can be accuractely estimated by using experimental results obtained by testing samples containing notches of two different sharpnesses. The accuracy and reliability of the proposed experimental methodology was checked by using a large amount of experimental results taken from the literature. Such a systematic validation exercise allowed us to fully confirm that the Theory of Critical Distances is not only an accurate static and fatigue assessment technique, but it can also be considered as an efficient experimental strategy suitable for estimating the classical Linear Elastic Fracture Mechanics material properties.

Keywords: Theory of Critical Distances, notches, threshold value of the stress intensity factor, plane strain fracture toughness

NOMENCLATURE

3PB	three point bending
4PB	four point bending
d_g, d_n	specimen's principal dimensions
r_n	notch root radius
t	thickness
AX	axial loading
CNP	central notch in a flat plate
CNB	circumferentially notched cylindrical bar
C(T)	compact specimen
D	notch depth
DC(T)	disk shaped compact specimen
DENP	double edge notch in a plate
F_u	ultimate force
L	material characteristic length
L_e	estimated value of the material characteristic length
L-S	L shaped specimen
K_{Ic}	plane strain fracture toughness
K_c	fracture toughness
$K_{Ic,e}$	estimated value of the plane strain fracture toughness
K_t	stress concentration factor
R	load ratio ($R=\sigma_{min}/\sigma_{max}$)
RB	rotating bending
SENP	single edge notch in a plate
UNCR	U-notched circular ring
σ_0	inherent material strength
$\sigma_{0,e}$	estimated inherent material strength
σ_1	maximum principal stress
σ_{UTS}	ultimate tensile strength
σ_Y	yield stress
σ_x, σ_y, σ_z,	normal stresses
τ_{xy}, τ_{xz}, τ_{yx},	shear stresses
r, θ	polar coordinates
ΔK_{th}	range of the threshold value of the stress intensity factor
$\Delta K_{th,e}$	estimated value of range of the threshold value of the stress intensity factor
$\Delta\sigma_0$	plain fatigue (or endurance) limit
$\Delta\sigma_{0n}$	notch fatigue limit referred to the gross section
$\Delta\sigma_1$	maximum principal stress range

INTRODUCTION

Thanks to its accuracy and reliability, nowadays Linear Elastic Fracture Mechanics (LEFM) is daily used by structural engineers engaged in performing the fatigue as well as the static assessment of real mechanical components. In particular, the range of the threshold value of the stress intensity factor, ΔK_{th}, and the plane strain fracture toughness, K_{Ic}, are those material constants used to evaluate the non-propagation of long cracks in engineering materials subjected to cyclic and static loading, respectively. In order to correctly determine the above material properties, the use of the procedures suggested by the available standard codes is always advisable (see, for instance, Refs [1,2]). However, as to the practical application of such techniques, it has to be admitted that a reliable determination of the LEFM material constants requires sophisticated equipment and a certain level of expertise on the part of the person responsible, and is, in any case, expensive and time-consuming. Moreover, very often it is not possible to produce specimens meeting, in terms of geometry and absolute dimensions, the requirements of the standard procedures themselves: for instance, in some circumstances it can be very difficult, in some cases impossible, to make specimens which are thick enough to meet the requirements for plane strain. This is especially true when considering that, to correctly take into account also the influence on the overall effect of the manufacturing processes, specimens may have to be machined out of real components.

Apart from the above practical problems which are daily encountered in industrial reality, it has to be said also that the scientific community seems not to always follow the recommendations of the available standard codes to determine such material properties for scientific purposes: sometimes, researchers adopt alternative strategies which depend not only on their in-field experience, but also on the type of testing facilities available in their laboratories (see, for instance, Ref. [3]).

In this complex scenario, and in light of the important role played by both K_{Ic} and ΔK_{th} in the static and fatigue assessment of real mechanical components, the present technical note aims to investigate the accuracy of the Theory of Critical Distances (TCD) in estimating the above material

properties from experimental results generated from relatively simple tests conducted on standard notches.

FUNDAMENTALS OF THE THEORY OF CRITICAL DISTANCES

The TCD was first proposed early in the last century by Neuber [4] and Peterson [5], respectively, to estimate the high-cycle fatigue strength of notched components. In more detail, Neuber has observed that notch fatigue limits could directly be predicted by averaging over a line the stress acting on the fatigue process zone, where the length of the integration domain depends on the fatigue properties of the material to be assessed [4]. Peterson instead has argued that the stress at a given distance from the stress concentrator apices could directly be used to perform the fatigue assessment of notched metallic materials [5].

Since the pioneering work done by the above two researchers, the TCD has continuously been rediscovered over the last century, proving to be highly accurate when used in different ambits of the structural integrity discipline [6]. For instance, in 1974 Whitney and Nuismer [7] have observed that the material characteristic length to be used to perform the static assessment of notched fibre composites could efficiently by calculated by directly combining the material toughness and the ultimate tensile strength. More recently, Tanaka [8] and Taylor [9] independently have proven that the same idea based on the LEFM concepts could be used also to estimate notch fatigue limits of conventional metal components.

Examination of the state of the art shows that the TCD can be formalised in different ways, which include the Point, Line, Area and Volume method. In particular, the Point Method (PM) postulates that a notched component is at its fatigue limit when the range of the linear-elastic maximum principal stress at a given distance from the stress raiser apex equals the material plain fatigue limit, $\Delta\sigma_0$, i.e. (Figures 1a and 1b) [8,9]:

$$\Delta\sigma_1\left(\theta=0, r=\frac{L}{2}\right)=\Delta\sigma_0 \tag{1}$$

In the above identity, L is the so-called material characteristic length which is defined as follows [8-10]:

$$L=\frac{1}{\pi}\left(\frac{\Delta K_{th}}{\Delta\sigma_0}\right)^2, \tag{2}$$

where both $\Delta\sigma_0$ and ΔK_{th} have to be determined at the same load ratio, R, as the one characterising the load history applied to the component to be assessed.

Similarly, under static loading the material characteristic length takes on the following value [7,11,12]:

$$L=\frac{1}{\pi}\left(\frac{K_{Ic}}{\sigma_0}\right)^2, \tag{3}$$

In the above definition, σ_0 is the inherent strength, that is, a material property whose definition varies as the type of material to be assessed changes [6]. For instance, when final breakage is preceded by a limited amount of plastic deformation, σ_0 is seen to be larger than the corresponding ultimate tensile stress. Brittle and quasi-brittle materials instead have inherent material strength equal to the ultimate tensile stress, σ_{UTS}. Finally, σ_0 is seen to be different from σ_{UTS} also in those situations in which the breakage of the plain material occurs by different mechanisms to those governing failures in the presence of stress concentration phenomena. If the L value of the material to be assessed is known from the experiments, the TCD can directly be used to perform the static assessment of notched components. In particular, the PM postulates that static breakage occurs

when the linear-elastic maximum principal stress at a distance from the notch of L/2 equals the inherent material strength (Figures 1a and 1c), that is [11,12]:

$$\sigma_1\left(\theta=0, r=\frac{L}{2}\right)=\sigma_0 . \quad (4)$$

Over the last decade, we have made a big effort to check the accuracy of the TCD (and, in particular, of the PM) in estimating static and fatigue strength of notched components. In more detail, when applied to assess conventional engineering materials containing different geometrical features, this theory was seen to be capable of predictions falling within an error interval equal to about ±20% [6, 11-16].

A logical extension of such an approach, though one which has not thus far been attempted, is that experimental data from plain and notched test specimens could, when analysed using the TCD, allow one to estimate the values of the LEFM constants ΔK_{th} and K_{Ic}. The aim of the present work was to investigate whether this could be done, for a range of engineering materials, with sufficient accuracy to allow it to be proposed as a viable alternative to the existing standard methods.

ON THE EXPERIMENTAL DETERMINATION OF K_{Ic} AND ΔK_{th} ACCORDING TO THE POINT METHOD

The way the PM works in practice suggests that both ΔK_{th} and K_{Ic} can be attempted to directly be evaluated from the linear-elastic stress fields acting on the material in the vicinity of stress raiser apices. In more detail, initially assume that, for the investigated material, the plain fatigue limit, $\Delta\sigma_0$, as well as a fatigue limit generated by testing samples containing a known geometrical feature, $\Delta\sigma_{0n}$, are known from the experiments (Fig. 2). Moreover, the above two fatigue limits must be determined at the same load ratio, R, as the one at which the range of the threshold value of the

stress intensity factor has to be estimated. By using either numerical or analytical methods, the linear-elastic stress field can now be plotted along the bisector of the notch used to determine $\Delta\sigma_{0n}$ (Fig. 2b). According to the schematic chart sketched in Figure 2b, the point at which the straight horizontal line corresponding to $\Delta\sigma_0$ and the above stress-distance curve intersect with each other allows the value of L/2 to directly be determined. Finally, according to Eq. (2), ΔK_{th} can be estimated as follows:

$$\Delta K_{th} = \Delta\sigma_0 \sqrt{\pi L} \, . \tag{5}$$

As to the expected accuracy of this approach [13-15], in theory, reliable estimates of ΔK_{th} are expected to be obtained independently of the type of the considered notch (i.e., short, sharp or blunt) [14], though it is clear that better accuracy will be achieved if $\Delta\sigma_{0n}$ is obtained by testing stress raisers as sharp as possible, since these features will be more "crack-like" and will, crucially, have a higher stress gradient, making it easier to accurately determine the point of intersection.

A similar strategy can be followed also to determine K_{Ic}, provided that, the value of the inherent material strength is known *a priori*. Unfortunately, as said above, the definition of σ_0 changes as the type of material to be assessed varies [6], so that, the plane strain fracture toughness is always suggested to be estimated by using, at least, two experimental results generated by testing samples containing notches having different sharpness. Assume then that the static strength of two notched geometries is known from the experiments. The linear-elastic stress fields in the vicinity of the considered stress raisers can now be plotted, in incipient failure condition, in a unique chart, determining the point at which the above two stress-distance curves intersect with each other: the coordinates of such a point allow both σ_0 and L/2 to directly be determined (Fig. 3). Finally, from the calculated value of the material characteristic length, L, the plane strain fracture toughness can be estimated as follows:

$$K_{Ic} = \sigma_0 \sqrt{\pi L}\,. \tag{6}$$

As with the determination of the fatigue threshold, it is advisable if one of the notches tested is as sharp as possible, though the type of notch which can be produced using normal machining methods is invariably sufficient. Moreover, due to the fact that, for certain materials, σ_0 is seen to be larger than the corresponding σ_{UTS}, the values of the stress concentration factor, K_t, of the specimens used to estimate K_{Ic} according to the procedure sketched in Figure 3 should always assure the following condition:

$$K_t > \frac{\sigma_0}{\sigma_{UTS}}. \tag{7}$$

Specimens tested in tension which have K_t less than the value specified by equation 7 will generally fail when the net section stress is similar to σ_{UTS}, i.e. the notch will have a negligible weakening effect, so another check on the correct value of K_t is that the nominal net-section stress to failure should be significantly less than σ_{UTS}.

VALIDATION BY EXPERIMENTAL DATA

In order to check the PM's accuracy in estimating both ΔK_{th} and K_{Ic}, several experimental results were selected from the technical literature. The sketches of the considered notched samples are reported in Figure 4. Table 1 summarises the error made when using, according to the procedure shown in Figure 2, the PM to evaluate ΔK_{th}. In the above table, for any considered material, the relevant dimensions of the used notched geometries are reported together with the corresponding value of the nominal notch fatigue (or endurance) limits, $\Delta\sigma_{0n}$. It is worth noticing here that

endurance limits were, in general, extrapolated in the range $2 \cdot 10^6$-10^7 cycles to failure. The type of applied loading as well as the investigated load ratio, R, are also clearly indicated in the above Table. The values of both L and ΔK_{th} were estimated by determining the linear-elastic stress fields acting on the material in the vicinity of the considered stress raisers through the FE method by gradually refining the mesh until convergence occurred. Finally, the error was calculated as follows:

$$\text{Error } [\%] = \frac{\text{experimental value} - \text{estimated value}}{\text{estimated value}} \cdot 100 \tag{8}$$

Table 1 makes it evident that the systematic use of the PM resulted in satisfactory estimates when compared with values of the threshold obtained using standard test methods, allowing 80% of the considered data to fall within an error interval of ±15%, 90% of the predictions being in the range ±20%.

Tables 2 and 3 show the accuracy of the PM in evaluating, according to the strategy summarised in Figure 3, the plane strain fracture toughness, K_{Ic}, of different engineering materials. In the above Tables also the relevant dimensions of the considered notched samples together with the corresponding experimental values of either the ultimate force, F_u, or the fracture toughness, K_c, are reported. For the materials listed in Table 2, both σ_0, L and K_{Ic} were estimated by post-processing the linear-elastic stress fields determined from refined FE models. On the contrary, due to a lack in the original sources of those pieces of information necessary to estimate the stress fields by using the FE method, the predictions summarised in Table 3 were made by following a different strategy [6]. In particular, the relevant stress-distance curves to be used to estimate both L and σ_0 were determined by taking full advantage of the Creager and Paris equation, i.e. [53, 54]:

$$\sigma_1(\theta = 0°, r) = \frac{K_c}{\sqrt{\pi}} \frac{2(r + r_n)}{(2r + r_n)^{\frac{3}{2}}} \tag{9}$$

It is possible to conclude the present section by observing that the error values listed in Tables 2 to 3 and calculated according to Eq. (8) seem to strongly support the idea that, in spite of the simplifications adopted to estimate the relevant stress-fields in some of the considered notched geometries, the usage of the PM (Fig. 3) resulted in 90% of the estimates falling within an error interval of ±15%.

DISCUSSION

The above exercise has demonstrated that this approach is capable of estimating fracture toughness and fatigue threshold values with good accuracy. The original sources for the experimental data which we used did not in general contain any information about the statistical dispersion of the results, however it is reasonable to suppose that values of these quantities measured using standard methods would show scatter of the order of 10-20%, which is similar to the prediction errors reported above. Indeed, the determination of ΔK_{th} is particularly prone to error, even when the standards are adhered to [62]. This has lead some researchers to propose that ΔK_{th} is not really an inherent material parameter and promoted others to search for new, more sophisticated ways of measuring the crack propagation threshold to avoid experimental artefacts [63].

Further discussion on this interesting topic is beyond the limits of this short technical note, whose aim was merely to demonstrate that results of comparable accuracy can be obtained using data from experiments which are much simpler to perform, requiring less sophisticated equipment and minimal expertise. The only additional requirement is a finite element analysis (or other stress-field analysis) of the component, but this can be achieved very simply using standard software and such results are indeed already available for many standard specimen geometries.

.

CONCLUSIONS

1) The TCD, applied in the form of the PM, was seen to be an efficient engineering tool suitable for estimating both ΔK_{th} and K_{Ic};
2) More work needs to be done in this area to standardise the optimum notched geometries to be used to estimate ΔK_{th} and K_{Ic} according to the strategy discussed in the present technical note.

REFERENCES

[1] Anon. Standard Test Method for Plane-Strain Fracture Toughness of Metallic Materials. ASTM E399, 1990 (Reapproved 1997).

[2] Anon. Standard Test Method for measurement of Fatigue Crack Growth Rates. ASTM E647, 2000.

[3] Lee YL, Pan J, Hathaway RB, Barkey ME. Fatigue Testing and Analysis (Theory and Practice). Elsevier Butterworth–Heinemann, Oxford, UK, 2005.

[4] Neuber H. Theory of notch stresses: principles for exact calculation of strength with reference to structural form and material. Springer Verlag, Berlin, II Ed. 1958.

[5] Peterson RE. Notch Sensitivity. In: Sines G., Waisman J. L., Editors. Metal Fatigue. New York. McGraw Hill 1959;293-306.

[6] Taylor D. The Theory of Critical Distances: A new perspective in fracture mechanics. Elsevier 2007.

[7] Whitney JM, Nuismer RJ. Stress fracture criteria for laminated composites containing stress concentrations. Journal of Composite Materials 1974;8:253-265.

[8] Tanaka K. Engineering formulae for fatigue strength reduction due to crack-like notches. Int. J Fracture 1983;22:R39-R45.

[9] Taylor D. Geometrical effects in fatigue: a unifying theoretical model. Int. J. Fatigue 1999;21:413-420.

[10] El Haddad MH, Topper TH, Smith KN. Fatigue crack propagation of short cracks. J. Engng. Mater. Tech. (ASME Trans.) 1979;101:42-45.

[11] Taylor D. Predicting the fracture strength of ceramic materials using the theory of critical distances. Eng Frac Mech 2004;71:2407-2416.

[12] Taylor D, Merlo, M, Pegley R, Cavatorta MP. The effect of stress concentrations on the fracture strength of polymethylmethacrylate. Material Science and Engineering 2004;A382: 288-294.

[13] Taylor D, Wang G. The validation of some methods of notch fatigue analysis. Fatigue Fract Engng Mater Struct 2000;23:387–394.

[14] Taylor D. A mechanistic approach to critical-distance methods in notch fatigue. Fatigue Fract Engng Mater Struct 2001;24:215-224.

[15] Susmel L, Taylor D. Fatigue Design in the Presence of Stress Concentrations. Int J of Strain Analysis for Engng Components 2003;38:443-452.

[16] Taylor D, Bologna P, Bel Knani K. Prediction of fatigue failure location on a component using a critical distance method. Int J Fatigue 2000;22:735-742.

[17] Taylor D, Hughest M, Allen D. Notch fatigue behaviour in cast irons explained using a fracture mechanics approach. Int J Fatigue 1996;18 7:439-445.

[18] Gasparini E,Meneghetti G. Una banca dati sul comportamento a fatica delle ghise sferoidali austemperate. La Metallurgia Italiana 2002; 3:29-35 (in Italian).

[19] Chapetti MD. High-cycle fatigue of austempered ductile iron (ADI). Int J Fatigue 2007;29:860–868.

[20] DuQuesnay DL, Topper TH, Yu MT. The effect of notch radius on the fatigue notch factor and the propagation of short cracks. In: The Behaviour of Short Fatigue Cracks, EGF Publication 1 (Edited by K. J. Miller and E. R. de Los Rios), Mechanical Engineering Publications, London, 1986, pp. 323–335.

[21] DuQuesnay DL, Yu MT, Topper TH. An analysis of notch size effect on the fatigue limit. J Testing Eval 1988;4:375-385.

[22] Tanaka K, Nakai Y. Propagation and non-propagation of short fatigue cracks at a sharp notch. Fatigue Fract. Engng. Mater. Struct. 1983;6:315-327.

[23] Tanaka K, Akiniwa Y. Notch geometry effect on propagation threshold of short fatigue cracks in notched components. In: Fatigue ’87, Vol. II (Edited by R. O. Ritchie, E. A. Starke Jr), Third International Conference on Fatigue and Fracture Thresholds, Charlottesville, VA, 1987, pp. 739-748.

[24] Frost NE. A relationship between the critical alternating propagation stress and crack length for mild steel. Proc. Inst. Mech. Engrs 1959;173:811-834.

[25] Harkegard G. An effective stress intensity factor and the determination of the notched fatigue limit. In: Fatigue Thresholds: Fundamentals and Engineering Applications, Vol. II (Ed. by J. Backlund, A. F. Blom and C. J. Beevers), Chameleon Press Ltd, London, 1981, pp. 867-879.

[26] Frost NE. Non-Propagating Cracks in Vee-Notched Specimens Subjected to Fatigue loadings. The Aeronautical Quarterly 1957;VIII:1-20.

[27] Lukas P, Kunz L, Weiss B, Stickler R. Non-damaging notches in fatigue. Fatigue Fract Engng Mater Struct 1986;9:195-204.

[28] Ting JC, Lawrence FV. A crack closure model for predicting the threshold stresses of notches. Fatigue Fract Engng Mater Struct 1993;16:93-114.

[29] Atzori B, Lazzarin P, Meneghetti G. Estimation of fatigue limits of sharply notched components. In: Proc. of Fatigue 2006, Atlanta, Georgia, USA, 2006.

[30] Usami S. Short Crack Fatigue Properties and Component Life Estimation, In: Current Research on Fatigue Cracks Vol. I, Elsevier Applied Science, 1987, pp. 119-147.

[31] Kihara S, Yoshii A. A strength evaluation method of a sharply notched structure by a new parameter, the equivalent stress intensity factor. JSME 1991;34:70-75.

[32] Atzori B, Lazzarin P, Meneghetti G. A unified treatment of the mode I fatigue limit of components containing notches or defects. Int J Fracture 2005;133:61-87.

[33] Yu MT, DuQuesnay DL, Topper TH. Notched fatigue behaviour of two cold rolled steels. Fatigue Fract Engng Mater Struct 1991;14 1:89-101.

[34] Chien CH, Coffin LF. A new method for predicting fatigue life in notched geometries. Fatigue Fract Engng Mater Struct 1998;21:1–15

[35] Glodez S, Potocnik R, Flasker J, Zafosnik B. Numerical modelling of crack path in the lubricated rolling–sliding contact problems. Eng Frac Mech 2008;75:880–891.

[36] Susmel L, Taylor D. A novel formulation of the Theory of Critical Distances to estimate Lifetime of Notched Components in the Medium-Cycle Fatigue Regime. Fatigue Fract Engng Mater Struct 2007;30 7:567-581.

[37] DuQuesnay DL, Abdel-Raouf H, Topper TH, Plumtree A. A modified fracture mechanics approach to metal fatigue. Fatigue Fract Engng Mater Struct. 1992;15:979-993.

[38] Fujimoto Y, Hamada K, Shintaku E, Pirker G. Inherent damage zone model for strength evaluation of small fatigue cracks. Eng Fract Mech 2001;68 4:455-473.

[39] Bian, JC, Tokaji K, Ogawa T. Notch sensitivity of aluminum-lithium alloys in fatigue. Fatigue Fract Engng Mater Struct 1995;18:119-127.

[40] El Haddad MH, Miettinen BI. Prediction of initiation and early fatigue crack growth in materials. In: Fatigue thresholds, Ed. by J. Backlund et alt., Vol. II, 1981, pp. 827-844.

[41] Zhao T, Zhang J, Jiang, Y. A study of fatigue crack growth of 7075-T651 aluminum alloy. Int J Fatigue 2008;30:1169-1180.

[42] Lazzarin P, Tovo R, Meneghetti G. Fatigue crack initiation and propagation phases near notches in metals with low notch sensitivity. Int J Fatigue 1997;19:647–657.

[43] Susmel, L., Taylor, D., Unpublished data.

[44] Dal Re V, Zucchelli A. Fracture toughness K_{IvM} measurement of non-brittle metallic materials by "Chevron Notched" specimens. In: Proceedings of XVII IGF Conference, Bologna, 16-18 June 2004 (ISBN 978-88-95940-16-8).

[45] Susmel L, Taylor D. On the use of the Theory of Critical Distances to predict static failures in ductile metallic materials containing different geometrical features. Eng Fract Mech 2008;75, 4410-4421.

[46] Strandberg M. Fracture at V-notches with contained plasticity. Eng Fract Mech 2002;69:403–415.

[47] El Minor H, Kifani A, Louah M, Azari Z, Pluvinage G. Fracture toughness of high strength steel—using the notch stress intensity factor and volumetric approach. Structural Safety 2003;25:35–45.

[48] Gómez FJ, Elices M. A fracture criterion for blunted V-notched samples. Int J Fracture 2004;127:239-264.

[49] Livieri P. Use of J-integral to predict static failures in sharp V-notches and rounded U-notches. Eng Fract Mech 2008;75:1779-1793.

[50] Susmel L, Taylor D. The theory of critical distances to predict static strength of notched brittle components subjected to mixed-mode loading. Eng Frac Mech, 2008;75 3-4:534-550.

[51] Zou Z, Fok SL, Oyadiji SO, Marsden BJ Failure predictions for nuclear graphite using a continuum damage mechanics model. Journal of Nuclear Materials 2004;324:116–124.

[52] Yosibash Z, Bussiba A, Gilad I. Failure criteria for brittle elastic materials. Int J Fracture 2004;125:307–333.

[53] Creager M, Paris PC. Elastic field equations for blunt cracks with reference to stress corrosion cracking. Int J Fract Mech 1967;3:247-252.

[54] Glinka G, Newport A. Universal features of elastic notchtip stress fields. Int J Fatigue 1987;9:143-150.

[55] Srinivas M, Kamat SV. Influence of temperature and notch root radius on the fracture toughness of a dispersion-strengthened aluminium alloy. Fatigue Fract Engng Mater Struct 2000;23:181-183.

[56] Tsuji K, Iwase K, Ando K. An investigation into the location of crack initiation sites in alumina, polycarbonate and mild steel. Fatigue Fract Engng Mater Struct 1999;22:509–517.

[57] Wilshaw TR, Rau CA, Tetelman AS. A general model to predict the elastic-plastic stress distribution and fracture strength of notched bars in plane strain bending. Eng Frac Mech 1968;1:191-211.

[58] Ritchie RO, Francis B, Server WL. Evaluation of toughness in AISI 4340 steel austenitised at low and high temperature. Metallurgical Transactions 1976;7A:831-838.

[59] Bertolotti RL. Fracture Toughness of polycrystalline alumina. Journal of the American Ceramic Society 1973;56:107-117.

[60] Takahashi I, Usami S, Nakakado H, Miyata H, Shida S. Effect of defect size and notch root radius on fracture strength of engineering ceramics. Journal of the Ceramic Society of Japan 1985;93:186-194.

[61] Usami S, Kimoto H, Takahashi I, Shida S. Strength of ceramic materials containing small flaws. Eng Frac Mech 1986;23:745-761.

[62] Newman JC Jnr, in: AGARD CP-328 (1983) 6.1-6.26

[63] Newman JC Jnr, Schneider J, Daniel A, McKnight D. Compression pre-cracking to generate near threshold fatigue-crack-growth rates in two aluminum alloys. Int J Fatigue 2005;27:1432-1440.

List of Captions

Table 1: PM's accuracy in estimating ΔK_{th}.
Table 2: PM's accuracy in estimating K_{Ic} by determining the relevant stress fields through the FE method.
Table 3: PM's accuracy in estimating K_{Ic} by determining the relevant stress fields through Creager and Paris' equation.

Figure 1: Adopted frame of reference and polar coordinates (a). The PM to estimate high-cycle fatigue (b) and static strength (c) of notched components.
Figure 2: The PM to estimate the range of the threshold value of the stress intensity factor, ΔK_{th}.
Figure 3: The PM to estimate the plane strain fracture toughness, K_{Ic}.
Figure 4: Investigated notched geometries.

Tables

	Material	σ_Y [MPa]	σ_{UTS} [MPa]	Ref.	Geometry	D [mm]	d_n [mm]	d_g [mm]	r_n [mm]	β [º]	Load type	R	$\Delta\sigma_{0n}$ [MPa]	$\Delta\sigma_0$ [MPa]	L_e [mm]	$\Delta K_{th,e}$ [MPa $m^{1/2}$]	ΔK_{th} [MPa $m^{1/2}$]	Ref.	Error [%]
Cast Iron	Grey Iron	202	249	[17]	CNB	3.18	23.64	30	0.3	90	AX	-1	91.0	155	2.723	14.3	15.9	[16]	11.2
	Grey Iron	202	249	[17]	CNB	3.18	23.64	30	0.3	90	AX	0.1	60.0	99	2.963	9.6	11.2	[16]	16.7
	Grey Iron	202	249	[17]	CNB	3.18	23.64	30	0.3	90	AX	0.5	44.0	68	3.542	7.2	8.0	[16]	11.1
	Grey Iron	202	249	[17]	CNB	3.18	23.64	30	0.3	90	AX	0.7	32.0	48	3.858	5.3	5.2	[16]	-1.9
	EN-GJS-800-8	-	-	[18]	DENP	1	18	20	0.1	90	AX	0.1	98.6	440	0.075	6.8	8.1	[17]	19.1
	ADI ASTM 897M-90	750	1020	[19]	CNB	1	7.5	9.5	0.5	-	RB	-1	226.3	880	0.134	18.1	18.5	[18]	2.2
Steel	SAE 1045	466	745	[20]	CNP	-	43.95	44.45	0.5	-	AX	-1	273.0	608	0.154	13.3	13.9	[19]	4.5
	SAE 1045	466	745	[21]	CNP	-	43.95	44.45	0.25	-	AX	0	308.0	448	0.158	9.3	6.9	[20]	-25.8
	G40.11 Steel	376		[21]	CNP	-	69.6	70	0.2	-	AX	-1	336.0	540	0.170	12.5	11.5	[20]	-8.0
	SM41B	194	423	[22,23]	CNP	3	39	45	0.16	-	AX	-1	95.3	326	0.346	10.7	12.4	[21,22]	15.5
	SM41B	194	423	[22,23]	CNP	3	39	45	0.16	-	AX	0	63.3	274	0.219	7.2	8.4	[21,22]	16.1
	SM41B	194	423	[22,23]	CNP	3	39	45	0.16	-	AX	0.4	73.0	244	0.361	8.2	6.4	[21,22]	-22.2
	Mild Steel	334	440	[24]	DENP	5.08	53.34	63.5	0.1	55	AX	-1	84.1	420	0.315	13.2	12.8	[24]	-3.0
	NiCr Steel (EN 26)	820	957	[26]	CNB	5.08	32.84	43	0.05	55	AX	-1	41.7	1000	0.085	16.4	12.8	[24]	-22.0
	Steel 15313	380	530	[27]	CNB	0.03	4.94	5	0.03	-	AX	-1	429.0	440	0.214	11.4	12.0	[26]	5.3
	AISI 304	222	-	[28]	CNB	5.08	32.84	43	0.05	55	AX	-1	72.3	720	0.110	13.4	12.0	[24]	-10.4
	FeP04	185	310	[29]	DENP	10	30	50	0.16	45	AX	0.1	45.4	247	0.813	12.5	10.0	[28]	-20.0
	HT60	-	-	[30]	DENP	0.5	50	51	0.05	90	AX	0	252.0	580	0.160	13.1	13.0	[29]	-0.8
	SS41	323	448	[31]	DENP	10	30	50	0.1	90	AX	0.05	25.9	231	0.211	6.0	6.4	[31]	6.7
	HT60 (2)	510	598	[31]	DENP	10	30	50	0.1	90	AX	0.05	31.0	425	0.083	6.9	6.6	[30]	-4.3
	SAE 1010-HR	-	326	[33]	CNP	-	43.45	44.45	0.5	-	AX	-1	220.7	320	0.570	13.5	11.8	[32]	-12.6
	SAE 1010-CR22	-	476	[33]	CNP	-	43.45	44.45	0.24	-	AX	-1	308.3	410	0.176	9.6	10.2	[32]	6.3
	SAE 1010-CR56	-	535	[33]	CNP	-	43.45	44.45	0.24	-	AX	-1	339.1	546	0.101	9.7	8.4	[32]	-13.4
	SAE 1010-CR76	-	689	[33]	CNP	-	43.45	44.45	0.24	-	AX	-1	363.3	614	0.088	10.2	6.4	[32]	-37.3
	SAE 945X-HR	-	58	[33]	CNP	-	43.45	44.45	0.24	-	AX	-1	390.6	500	0.199	12.5	13.4	[32]	7.2
	SAE 945X-CR30	-	621	[33]	CNP	-	43.45	44.45	0.24	-	AX	-1	374.5	588	0.088	9.8	12.4	[32]	26.5
	SAE 945X-CR61	-	752	[33]	CNP	-	43.45	44.45	0.24	-	AX	-1	406.5	630	0.113	11.9	12.0	[32]	0.8
	SAE 4130	-	-	[34]	DENP	9.525	38.1	57.15	1.45	-	AX	-1	93.3	610	0.053	7.9	8.5	[34]	7.6
	En3B	606	638	[36]	SENP	4	21	25	0.12	60	AX	-1	103.4	412	0.496	16.3	16.2	[35]	-0.6
	En3B	606	638	[36]	SENP	4	21	25	0.12	60	AX	0.1	75.0	328	0.416	11.9	11.8	[35]	-0.8

Table 1: PM's accuracy in estimating ΔK_{th} (continued).

	Material	σ_Y [MPa]	σ_{UTS} [MPa]	Ref.	Geometry	D [mm]	w_n [mm]	w_g [mm]	r_n [mm]	β [°]	Load type	R	$\Delta\sigma_{0n}$ [MPa]	$\Delta\sigma_0$ [MPa]	L_e [mm]	$\Delta K_{th,e}$ [MPa $m^{1/2}$]	ΔK_{th} [MPa $m^{1/2}$]	Ref.	Error [%]
Aluminium	2024-T351	360	466	[21]	CNP	-	44.21	44.45	0.12	-	AX	-1	159.0	248	0.112	4.6	4.4	[36]	-4.3
	2024-T351	360	466	[21]	CNP	-	43.95	44.45	0.25	-	AX	0	113.0	172	0.119	3.3	3.4	[36]	3.0
	AL-B.S.L. 65	425	486	[26]	CNB	5.08	33.02	43.18	0.203	55	AX	-1	26.8	300	0.059	4.1	4.2	[27]	2.4
	2024-T3	-	-	[34]	DENP	9.525	38.1	57.15	1.45	-	AX	-1	43.2	231	0.380	7.7	6.4	[37]	-16.9
	2024-T4	419	551	[39]	CNB	1	8	10	0.3	60	RB	-1	60.0	180	0.271	5.3	5.5	[39]	3.8
	7075-T6511	610	659	[39]	CNB	1	8	10	0.3	60	RB	-1	100.0	260	0.364	8.8	9.2	[40]	4.5
	AL 356-T6	-	182	[42]	DENP	8	24	40	0.1	-	AX	0.1	29.2	140	0.530	5.7	5.0	[31]	-12.3

Table 1: PM's accuracy in estimating ΔK_{th}.

	Material	σ_Y [MPa]	σ_{UTS} [MPa]	Ref.	Geometry	D [mm]	w_n [mm]	w_g [mm]	r_n [mm]	β [°]	t [mm]	Load type	F_{0n} [kN]	$\sigma_{0,e}$ [MPa]	L_e [mm]	$K_{Ic,e}$ [MPa $m^{1/2}$]	K_{Ic} [MPa $m^{1/2}$]	Ref.	Error [%]
Metals	Al6082	347	367	[43]	CNB	1.9	6.2	10	0.44	60	-	AX	16.2	445.9	1.636	32	35.8	[43]	11.9
					CNB	1.95	6.1	10	4	60	-	AX	13.1						
	En3B	606	638	[45]	DENP	3	19	25	0.1	60	6	AX	91.5	638	7.808	99.9	103.9	[44]	4.0
					SENP	5	20	25	3	0	6	3PB	33.0						
	AISI 01 (at -50° C)	501	-	[46]	SENP	5	25	30	≈0.08	0	16.6	AX	140.4	2753	0.114	52.2	52±2.8	[45]	-0.4
					SENP	5	25	30	≈0.08	140	16.6	AX	242.5						
	45SCD6	1463	1662	[47]	UNCR	4	20	40	0.15	0	7	AX	36.6	3346	0.32	106.1	97.0	[46]	-8.6
					UNCR	4	20	40	2	0	7	AX	45.3						
Polymers	PMMA (at -60°C)	-	128.4	[48]	SENP	14	14	28	2	0	14	3PB	1.18	155.1	0.026	1.4	1.7±0.1	[47]	21.4
					SENP	14	14	28	0.2	0	14	3PB	0.452						
	PMMA	-	100	[49]	DENP	6	18	30	5	0	6	AX	5.78	105.3	0.031	1.5	1.6	[48]	6.7
					DENP	6	18	30	1	0	6	AX	3.12						
	PMMA	-	67	[50]	DENP	2.3	8.2	12.8	0.2	60	0.75	AX	0.16	113.9	0.108	2.1	2.2	[6]	4.8
					DENP	2.3	8.2	12.8	0.4	60	0.75	AX	0.20						
	PVC	-	140	[49]	DENP	6	18	30	5	0	6	AX	7.51	135.1	0.097	2.4	2.6	[48]	8.3
					DENP	6	18	30	1	0	6	AX	4.67						
Ceramics	Nuclear graphite	-	33	[51]	L-S	-	21	54	2	45	15	AX	0.53	33	0.846	1.7	1.5	[50]	-14.7
					L-S	-	21	54	4	45	15	AX	0.61						
	Alumina-7% Zirconia	-	290	[52]	SENP	5	10	15	0.06	30	10	4PB	1.49	435	0.034	4.5	4.1	[51]	-8.9
					SENP	5	10	15	0.1	30	10	4PB	1.84						

Table 2: PM's accuracy in estimating K_{Ic} by determining the relevant stress fields through the FE method.

	Material	σ_Y [MPa]	σ_{UTS} [MPa]	Ref.	Geometry	r_n [mm]	β [°]	t [mm]	Load type	K_C [MPa $m^{1/2}$]	$\sigma_{0,e}$ [MPa]	L_e [mm]	$K_{Ic,e}$ [MPa $m^{1/2}$]	K_{Ic} [MPa $m^{1/2}$]	Ref.	Error [%]
Metals	Al Alloy DISPAL (at 25°C)	320	360	[55]	DC(T)	0.35	0	10	AX	22.2	1214	0.046	14.6	13.0	[54]	-11.0
					DC(T)	0.16	0	10	AX	16.7						
	Al Alloy DISPAL (at 150°C)	265	293	[55]	DC(T)	0.5	0	10	AX	21.1	940	0.068	13.7	10.5	[54]	-23.4
					DC(T)	0.16	0	10	AX	14.8						
	Al Alloy DISPAL (at 250°C)	210	223	[55]	DC(T)	0.5	0	10	AX	17.9	816	0.054	10.6	9.0	[54]	-15.1
					DC(T)	0.16	0	10	AX	10.8						
	Al Alloy DISPAL (at 350°C)	161	173	[55]	DC(T)	0.5	0	10	AX	13.0	560	0.088	9.3	7.9	[54]	-15.1
					DC(T)	0.16	0	10	AX	8.9						
	JIS G3106 SM400C (at -170°C)	700	810	[56]	SENP	0.5	0	30	3PB	55.7	2562	0.049	31.8	32.0	[55]	0.6
					SENP	1	0	30	3PB	75.3						
	Mild Steel (at -196°C)	827	1379	[57]	SENP	0.25	45°	10	3PB	36.2	2247	0.038	24.6	23.6	[56]	-4.1
					SENP	0.73	45°	10	3PB	56.6						
	AISI 4340 (small grain size)	1593	2217	[58]	C(T)	0.04	0	15.4	AX	51.8	8524	0.005	34.5	36.0	[57]	4.3
					C(T)	0.32	0	15.4	AX	147.8						
	AISI 4340 (large grain size)	1593	2193	[58]	C(T)	0.22	0	15.4	AX	56.4	3016	0.097	52.5	55.5	[57]	5.7
					C(T)	0.6	0	15.4	AX	58.5						
Ceramics	Alumina	-	297	[56]	SENP	1	0	10	3PB	9.4	322	0.035	3.4	3.8	[55]	11.8
					SENP	0.26	0	10	3PB	5.2						
	Alumina (at 1000°C)	-	215	[56]	SENP	0.11	0	10	3PB	3.2	263	0.034	2.7	2.2	[55]	-20.4
					SENP	0.5	0	10	3PB	5.6						
	Alumina	-	-	[59]		0.5				7.7	374	0.02	2.9	3.1	[58]	6.9
						1				10.7						
	Silicon Nitride	-	550	[60, 61]		0.01				5.3	710	0.021	5.8	5.0	[59, 60]	-13.8
						0.05				6.2						
	Silicon Carbide	-	620	[60, 61]		0.01				3.8	768	0.008	3.9	3.7	[59, 60]	-5.1
						0.12				8.0						
	Polycarbonate	67.9	70.2	[56]	C(T)	0.5	0	15	AX	5.5	234	0.093	4.0	3.4	[55]	-15.0
					C(T)	2.4	0	15	AX	10.5						

Table 3: PM's accuracy in estimating K_{Ic} by determining the relevant stress fields through Creager and Paris' equation.

Figures

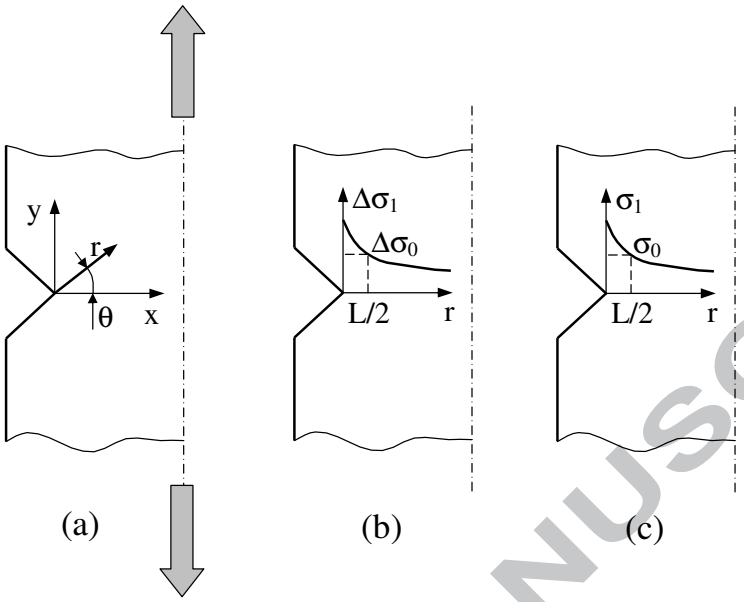

Figure 1: Adopted frame of reference and polar coordinates (a). The PM to estimate high-cycle fatigue (b) and static strength (c) of notched components.

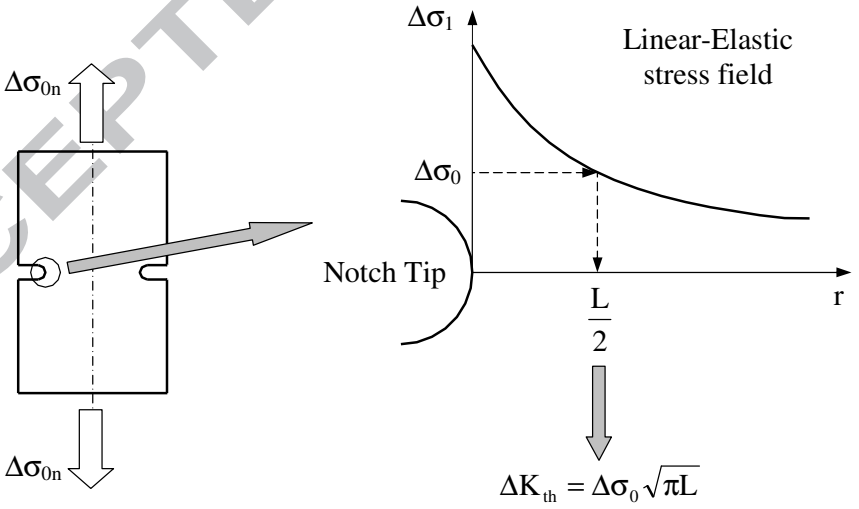

Figure 2: The PM to estimate the range of the threshold value of the stress intensity factor, ΔK_{th}.

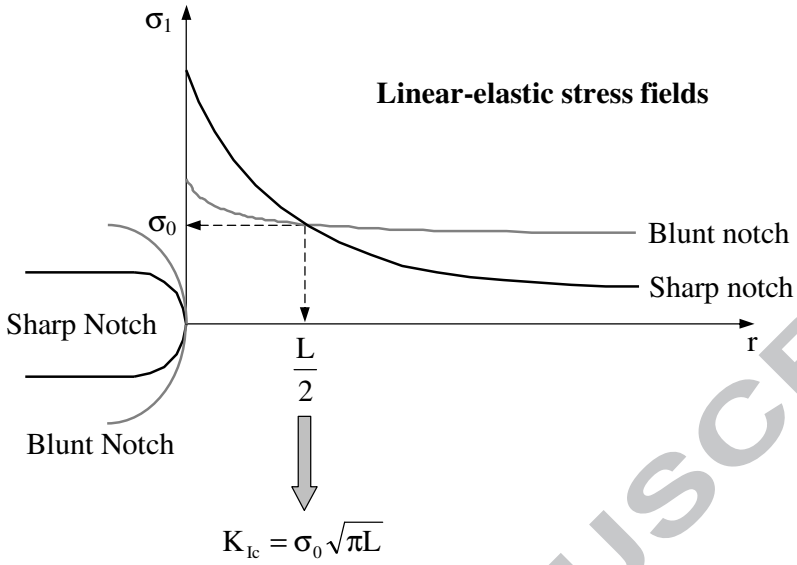

Figure 3: The PM to estimate the plane strain fracture toughness, K_{Ic}.

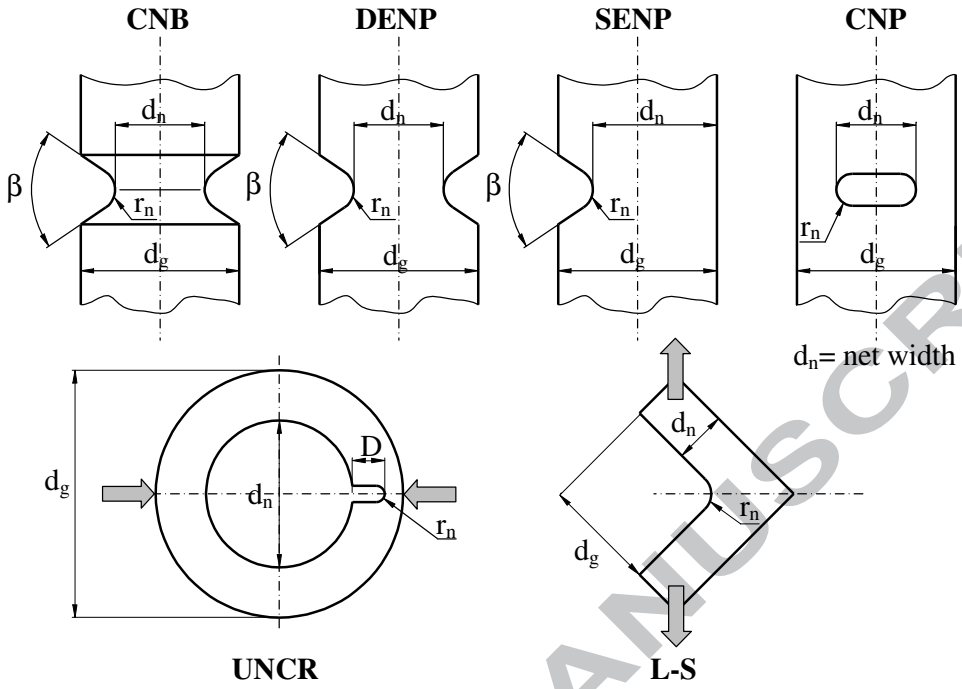

Figure 4: Investigated notched geometries.